Performance Analysis of Two-Way Relay NOMA Systems with Hardware Impairments and Channel Estimation Errors

**Xinji Tian[1], Qianqian Li[1], Xingwang Li[1], Hui Zhang[2*], Khaled Rabie[3]
and Charles Casimiro Cavalcante[4]**

[1] School of Physics and Electronic Information Engineering, Henan Polytechnic University, Jiaozuo, 454000, China
[e-mail: tian215216@sohu.com, liqianqian_lf@163.com, lixingwang@hpu.edu.cn]
[2] School of Energy Science and Engineering, Henan Polytechnic University, Jiaozuo, 454000, China
[e-mail: caikuangzhang@163.com]
[3] School of Electrical Engineering, Manchester Metropolitan University, Manchester M1 7JW, K.
[e-mail:k.rabie@mmu.ac.uk]
[4] Wireless Telecommunications Research Group, Federal University of Ceará, Campus do Pici, Bl. 722, ZIP
60455-760, Fortaleza-CE, Brazil
[e-mail: charles@gtel.ufc.br]
[*]Corresponding author: Hui Zhang

Abstract

In this paper, we consider a two-way relay non-orthogonal multiple access (TWR-NOMA) system with residual hardware impairments (RHIs) and channel estimation errors (CEEs), where two group users exchange their information via the decode-and-forward (DF) relay by using NOMA protocol. To evaluate the performance of the considered system, exact analytical expressions for the outage probability of the two groups users are derived in closed-form. Moreover, the asymptotic outage behavior in the high signal-to-noise ratio (SNR) regime is examined and the diversity order is derived and discussed. Numerical simulation results verify the accuracy of theoretical analyses, and show that: *i)* RHIs and CEEs have a deleterious effects on the outage probabilities; *ii)* CEEs have significant effects on the performance of the near user; *iii)* Due to the RHIs, CEEs, inter-group interference and intra-group interference, there exists error floors for the outage probability.

Keywords: Non-orthogonal multiple access, residual hardware impairments, two-way relay, channel estimation errors.

1. Introduction

Non-orthogonal multiple access (NOMA) has been identified as a promising technique for the fifth generation (5G) mobile communication network since it has the advantages of low latency, massive connectivity and high spectral efficiency [1-3]. In general, NOMA can be classified into two categories: power domain NOMA [4] and code domain NOMA [5]. For power domain NOMA, multi-users can be simultaneously served by the same base station using the same resource, while for code domain NOMA, the signals of different users are spread by using different codes and then multiplexed over the same time-frequency resources [6]. In this paper, we consider the power domain NOMA. It is worth noting that the power domain NOMA mentioned through this paper will be replaced by NOMA. For NOMA systems, in order to ensure a trade-off between throughput and user fairness, more powers are allocated to the users with poorer channel conditions. At the transmitter, the superposition signals are sent by power multiplexing, while the signals can be separately decoded at receivers by successive interference cancellation (SIC) [7].

Cooperative communication is another effective way to improve spectral efficiency, reduce transmit power and broaden the network coverage [8]. To further improve the system performance, two-way relay (TWR) was proposed for its ability to exchange information with the aid of a common relay with bidirectional information-transmission [9]. For combat channel fading and improve transmission reliability, the diversity behavior of the generalized MIMO TWR networks was studied in [10], where a two relay antenna selection (RAS) scheme was proposed. In [11], the outage behavior of a TWR network subject to a nonlinear transmission at the relay was studied, where fixed-gain and variable-gain amplify-and-forward (AF) relay were taken into account. Considering mixed asymmetric line-of-sight (LoS)/non-LoS (NLoS) fading scenario, the authors in [12] investigated the outage probability and channel capacity of the TWR networks. In [13], a distributed robust beamforming scheme was designed to minimize the total transmit power of the cognitive TWR networks. To further enhance the performance, the multi-antenna technique was introduced to the TWR networks [14], in which an optimal linear beamforming scheme was proposed to minimize the weighted mean squared error. As a further advance, massive multiple-input multiple-output (MIMO) inspired TWR network were involved in [15], where the impact of residual hardware impairments (RHIs) was investigated by considering Rician fading channels.

Recently, the combination of TWR and NOMA, known as TWR-NOMA, has drawn a considerable research attention, since it exploits advantages of both TWR and NOMA [16–19]. In [16], the outage probability and ergodic rates of a TWR-NOMA system were investigated, in which perfect and imperfect SIC were analyzed. Sparked by full-duplex, the authors in [17] proposed a full duplex cooperative NOMA system, the outage probability and ergodic capacity of the proposed system were derived. For increase the system throughput and reduce the signaling overhead, the multi-pair TWR-NOMA network were developed in [18], in which an optimal group decoding scheduling scheme joint fair rate allocation was proposed for uplink and downlink. With the emphasis on secure transmission, different decoding schemes of the NOMA-based full-duplex TWR networks were proposed in [19] based on SIC for the legitimate users, relay and eavesdroppers.

Although the above-mentioned works provide a solid foundation on the TWR-NOMA systems, one of the limitations of the above works is that the perfect hardware is assumed. In practice, due to deploying low-cost and low power efficiency RF components, the transceivers

5372

Tian et al.: Performance Analysis of Two-Way Relay NOMA Systems
with Hardware Impair-ments and Channel Estimation Errors

are prone to hardware imperfections and impaired by some types of hardware impairments, such as in-phase/quadrature-phase (I/Q) imbalance, amplifier non-linearities, and phase noise [20–22]. Although some signal processing algorithms can be used to compensate for the above imperfections, there still remains some RHIs due to estimation errors, inaccurate calibration and different types of noise [23], [24]. As stated in [20] [22] [25], the RHIs have significant effects on the system performance. The authors in [20] quantified the aggregated impact of RHIs on dual-hop relaying systems. The joint impact of RHIs and imperfect CSI on the multi-relay NOMA system was investigated in [22]. The authors in [25] derived the expressions of outage probability and approximate ergodic sum rate for analysis the deleterious effect of RHIs on the dual-hop NOMA network. The performance of wireless communication systems in the presence of RHIs has been extensively studied, e.g., see [26–28] and the references therein. The authors in [26] analyzed the effect of RHIs on the ergodic channel and ergodic sum rates of optimal and linear minimum mean-square-error (MMSE) receivers of MIMO systems. In [27], authors investigated the lower bound for the achievable sum rate of regular and large-scale MIMO systems with zero-forcing receivers in the presence of RHIs. In [28], exact closed-form expressions of outage probability and asymptotic expressions were derived in a TWR cooperative network with opportunistic relay selection, and the allocation of the fixed hardware impairments are analyzed as well. Recently, there are some research works dealing with the performance analysis of related topics of NOMA with RHIs, e.g., [29–31]. In [29], the authors investigated the performance of the one way cooperative NOMA network with RHIs by deriving a closed-form expression for the outage probability. Considering RHIs at the relay, [30] derived analytical expressions for the outage probability and symbol error rate of a TWR network. In [31], a one way relay dual-hop NOMA network with RHIs at source, relay and destination was considered, in which the outage probability, asymptotic individual ergodic rate (IER) and ergodic sum rate (ESR) were obtained. Nevertheless, the above works assume that all nodes have perfect channel state information (CSI). In fact, the performance of wireless communication system is greatly affected by wireless channel, such as shadow fading and frequency selective fading, which makes the path between transmitter and receiver very complicated. Due to randomness nature of wireless channels, it is a great challenge to obtain perfect channel knowledge. The common way of doing this is to use some estimation algorithms to obtain the estimated. However, the perfect estimation is not available due to channel estimation errors (CEEs). Therefore, it is of significance to investigate the joint impact of RHIs and CEEs on the TWR-NOMA system.

Motivation and Contribution: Motivated by the above discussion, different from the existing works on TWR-NOMA systems, we investigate the performance of TWR-NOMA systems in the presence of RHIs and CCEs, where two groups NOMA users exchange their information with the aid of decode-and-forward (DF) relay. The contributions of this paper are summarized as follows:

- Contrary to the existing research works on the performance of TWR-NOMA, we consider two practical factors, namely, RHIS and CEE. We aim at investigating the joint effects of the two factors on TWR-NOMA networks, which is a valuable problem for practical system analysis and design.
- We derived exact closed-form analytical expressions for the outage probability of the far users and near users. In addition, we also derived exact analytical expressions for the outage probability of the considered network under the condition of ideal RF components and CSI.
- We examine the asymptotic outage behavior of the users and discuss the diversity order in the high signal-to-noise ratio (SNR) region. It reveals that RHIs and CEEs

can cause the outage performance to deteriorate. Moreover, the results show that there exists an error floor for the outage probability due to inter/intra group interference and CEEs, and the diversity order is zero. Additionally, CEEs have a deleterious effect on the outage probability on the near users.

Organization: The rest of this paper is organized as follows. In section II, we present the TWR-NOMA system model in the presence of RHIs and CEEs. The exact closed-form analytical and asymptotic expressions for the outage probability and diversity order are derived and discussed in section III. In section IV, we present some numerical and simulation results to verify the accuracy of our analysis. A brief summary of this paper is concluded in section V.

Notations: In this paper, the main notations are shown as follows: $E\{\cdot\}$ denotes the expectation operation, $\mathrm{Pr}(\cdot)$ is the probability, $\prod(\cdot)$ denotes the continuous multiplication operation, $\sum(\cdot)$ is the summation.

2. System Model

A TWR-NOMA system is considered, which consists of one two-antenna relay R and two groups of NOMA users $G_1 = \{U_1, U_2\}$ and $G_2 = \{U_3, U_4\}$ as illustrated in **Fig. 1**. For NOMA users, we assume that two types of users are deployed: U_1 and U_3 are the near users, and U_2 and U_4 are the far users. The users of same type aim to exchange their informations via a two-antenna relay R, namely R_1 and R_2. In addition, there is no direct link between two groups of users due to heavy shadowing. We also assume that all users are equipped with a single antenna and operate in a half-duplex mode. h_i, $i \in \{1, 2, 3, 4\}$, denotes the channel fading coefficients between U_i and R, where h_i follows independent Rayleigh random variables with $|h_i|^2 \sim CN(0, \delta_i^2)$.
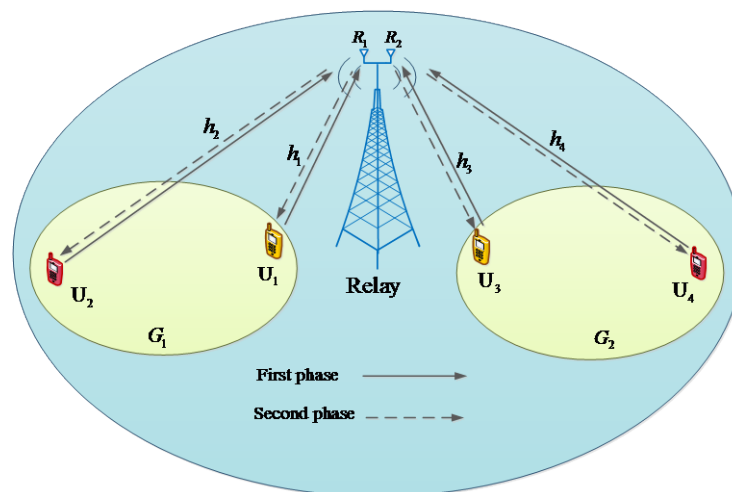

Fig. 1. System model

In practice communication systems, it is a great challenge to obtain perfect CSI due to the CEEs. Thus, the channel fading coefficient can be modeled as $h_i = \hat{h}_i + e_i$, where $\hat{h}_i$ represent the estimated channels coefficient, e_i are the CEEs, which can be modeled by Gaussian random variable with $e_i \sim CN\left(0, \delta_{e_i}^2\right)$ [32].

The whole communication is completed in two phases: 1) multiple access channel (MAC) phase; 2) broadcasting (BC) phase.

1) MAC Phase: In this phase, two pairs of users simultaneously transmit the respective information to the intended antenna of the relay, and the received information at $R_1(R_2)$ suffers from interference from the users of $G_2(G_1)$. Thus, the received signals at R_1 and R_2 are respectively given by

$$y_{R_1} = h_1\sqrt{a_1 P_u}\,x_1 + h_2\sqrt{a_2 P_u}\,x_2 + \varpi_1 I_2 + \eta_r + n_{R_1} \tag{1}$$

$$y_{R_2} = h_3\sqrt{a_3 P_u}\,x_3 + h_4\sqrt{a_4 P_u}\,x_4 + \varpi_1 I_1 + \eta_r + n_{R_2} \tag{2}$$

where x_i are the transmitted signals by the user U_i, with $E\{x_i\} = 1$, $i \in \{1,2,3,4\}$. P_u is the transmission power. a_1, a_2, a_3 and a_4 are the corresponding power allocation coefficients, satisfying $a_1 > a_2$, $a_1 + a_2 = 1$, and $a_3 > a_4$, $a_3 + a_4 = 1$; I_2 is the inter-group interference signal (IS) from R_2 with $I_2 = h_3\sqrt{a_3 P_u}\,x_3 + h_4\sqrt{a_4 P_u}\,x_4$; $\varpi_1 \in [0,1]$ is the impact level of inter-group IS at R; I_1 is the inter-group IS from R_1 with $I_1 = h_1\sqrt{a_1 P_u}\,x_1 + h_2\sqrt{a_2 P_u}\,x_2$; n_{R_1} and n_{R_2} are additive white Gaussian noise (AWGN) with zero mean and N_0 variance at R_1 and R_2, respectively; η_r represents the received RHIs at relay with $\eta_r \sim CN\left(0, \kappa_r^2 P_u \sum_{i=1}^{4}|h_i|^2\right)$, κ_r is used to characterize the aggregated level of RHIs from the relay [33].

According to the DF protocol of NOMA, R_1 first decodes x_1 by treating signals from the users of another group as inter-group IS. Then, the received signal-to-interference plus noise rates (SINR) at R_1 to detect x_1 is given by

$$\gamma_{R \to x_1} = \frac{\rho_u \left|\hat{h}_1\right|^2 a_1}{\rho_u \left|\hat{h}_2\right|^2 a_2 + \sum_{k=1}^{4}\rho_u \left|\hat{h}_k\right|^2 \kappa_r^2 + \sum_{j=3}^{4}\rho_u \left|\hat{h}_j\right|^2 \varpi_1 a_j + \vartheta_1} \tag{3}$$

where $\vartheta_1 = \sum_{i=1}^{2}\rho_u \delta_{e_i}^2 a_i + \sum_{j=3}^{4}\varpi_1 \rho_u \delta_{e_j}^2 a_j + \sum_{k=1}^{4}\kappa_r^2 \rho_u \delta_{e_1}^2 + 1$, and $\rho_u = P_u/N_0$ denotes the transmit SNR at the user nodes.

Then, the SINR at relay to decode x_2 is given

$$\gamma_{R \to x_2} = \frac{\rho_u \left|\hat{h}_2\right|^2 a_2}{\sum_{k=1}^{4}\rho_u \left|\hat{h}_k\right|^2 \kappa_r^2 + \sum_{j=3}^{4}\rho_u \left|\hat{h}_j\right|^2 \varpi_1 a_j + \vartheta_1} \tag{4}$$

2) BC Phase: In this phase, the relay decodes and forwards the received signals to all users. More specifically, the antennas R_2 and R_1 send the superposed signals $\left(\sqrt{b_1 P_r}\,x_1 + \sqrt{b_2 P_r}\,x_2\right)$

and $\left(\sqrt{b_3 P_r} x_3 + \sqrt{b_4 P_r} x_4 \right)$ to G_2 and G_1, respectively, where P_r is the transmission power at the relay, b_1, b_2, b_3 and b_4 are the power allocation coefficients. According the NOMA protocol, the far users are allocated more power than the near users $b_2 > b_1$, with $b_1 + b_2 = 1$ and $b_4 > b_3$, with $b_3 + b_4 = 1$.

The received signals at U_3 and U_4 denoted by y_{U_3} and y_{U_4}, can be respectively expressed as

$$y_{U_3} = h_3 \left(\sum_{i=1}^{2} \sqrt{b_i P_r} x_i + \eta_t \right) + \varpi_2 h_3 \sum_{j=3}^{4} \sqrt{b_j P_r} x_j + n_3 \tag{5}$$

$$y_{U_4} = h_4 \left(\sum_{i=1}^{2} \sqrt{b_i P_r} x_i + \eta_t \right) + \varpi_2 h_4 \sum_{j=3}^{4} \sqrt{b_j P_r} x_j + n_4 \tag{6}$$

where $\varpi_2 \in [0,1]$ is the impact level of inter-group IS at the user nodes, n_3 and n_4 are AWGN with mean power N_0 at U_3 and U_4, respectively; η_t represents the RHIs at the relay transmitter node, $\eta_t \sim CN\left(0, \kappa_t^2 P_r\right)$, κ_t is used to characterize the aggregate level of impairments in the transmitter hardware.

We assume that the signals x_2 from the users can be correctly decoded at R in the MAC phase. U_3 decodes the desired signal x_1 after using SIC to decode and eliminate x_2. The effective SINR at U_3 for the detection of x_2 is given by

$$\gamma_{U_3 \to x_2} = \frac{\rho_r \left| \hat{h}_3 \right|^2 b_2}{\rho_r \left| \hat{h}_3 \right|^2 b_1 + \rho_r \left| \hat{h}_3 \right|^2 \kappa_t^2 + \varpi_2 \rho_r \left| \hat{h}_3 \right|^2 + \vartheta_2} \tag{7}$$

where $\vartheta_2 = \rho_r \delta_{e_3}^2 \left(1 + \kappa_t^2 + \varpi_2\right) + 1$, $\rho_r = P_r / N_0$ is the transmit SNR at the relay node.

Similarly, we assume that the signals x_1 from the users can be correctly decoded at R in the MAC phase. After SIC operations, the received SINR at U_3 to decode x_1 is given by

$$\gamma_{U_3 \to x_1} = \frac{\rho_r \left| \hat{h}_3 \right|^2 b_1}{\rho_r \left| \hat{h}_3 \right|^2 \kappa_t^2 + \varpi_2 \rho_r \left| \hat{h}_3 \right|^2 + \vartheta_2} \tag{8}$$

Then, the received SINR at U_4 to decode signal x_2 is given by

$$\gamma_{U_4 \to x_2} = \frac{\rho_r \left| \hat{h}_4 \right|^2 b_2}{\rho_r \left| \hat{h}_4 \right|^2 b_1 + \rho_r \left| \hat{h}_4 \right|^2 \kappa_t^2 + \varpi_2 \rho_r \left| \hat{h}_4 \right|^2 + \vartheta_3} \tag{9}$$

where $\vartheta_3 = \rho_r \delta_{e_4}^2 \left(1 + \kappa_t^2 + \varpi_2\right) + 1$. After these processes, the information is exchanged between the NOMA users in G_1 and G_2.

3. Outage Performance Analysis

In this section, we first derive the exact analytical expressions for the outage probability. Then the asymptotic outage behavior at high SNR region is analyzed, and the diversity orders are also discussed.

3.1 Exact Outage Probability

1) Outage probability for U_1

In the TWR-NOMA, the outage event of U_1 occurs in the following three cases: *i*) The information x_1 cannot be decoded by R_1; *ii*) U_3 cannot decode x_2 successfully; *iii*) The information x_1 cannot be decoded by U_3, while U_3 can first decode the information x_2 correctly. Hence, the outage probability of U_1 can be written as

$$P_{U_1}^{out} = 1 - \Pr\left(\gamma_{R \to x_1} > \gamma_{thf}\right) \Pr\left(\gamma_{U_3 \to x_2} > \gamma_{thm}, \gamma_{U_3 \to x_1} > \gamma_{thf}\right) \tag{10}$$

where $\gamma_{thf} = 2^{2R_f} - 1$, $\gamma_{thm} = 2^{2R_m} - 1$. R_f and R_m are the target rates at U_3 to detect x_1 and x_2, respectively.

Then, the outage probability of U_1 for the TWR-NOMA with RHIs and CEEs is provided in the following theorem.

Theorem 1. For the non-ideal cases $\left(\delta_{e_i}^2 \neq 0, \kappa_l \neq 0, i \in \{1, 2, 3, 4\}, l \in \{t, r\}\right)$, the closed-form expression for the outage probability of U_1 is expressed as

$$P_{U_1}^{ni,out} = 1 - e^{-\frac{\tau_0}{\hat{\delta}_3^2} - \frac{\theta_1 \vartheta_1}{\hat{\delta}_1^2}} \prod_{i=1}^{3} \lambda_i \left(\frac{\Phi_1 \hat{\delta}_1^2}{\lambda_1 \hat{\delta}_1^2 + \theta_1} - \frac{\Phi_2 \hat{\delta}_1^2}{\lambda_2 \hat{\delta}_1^2 + \theta_1} + \frac{\Phi_3 \hat{\delta}_1^2}{\lambda_3 \hat{\delta}_1^2 + \theta_1} \right) \tag{11}$$

where $\Phi_1 = \left(\lambda_2 - \lambda_1\right)^{-1}\left(\lambda_3 - \lambda_1\right)^{-1}$, $\Phi_2 = \left(\lambda_3 - \lambda_2\right)^{-1}\left(\lambda_2 - \lambda_1\right)^{-1}$, $\Phi_3 = \left(\lambda_3 - \lambda_1\right)^{-1}\left(\lambda_3 - \lambda_2\right)^{-1}$, $\theta_1 = \dfrac{\gamma_{thf}}{\rho_u \left(a_1 - \gamma_{thf} \kappa_r^2\right)}$ with $a_1 > \gamma_{thf} \kappa_r^2$, $\tau_0 = \max\left(\tau_2, \tau_1\right)$, where $\tau_1 = \dfrac{\gamma_{thf} \vartheta_2}{\rho_r \left(b_1 - \gamma_{thf}\left(\kappa_t^2 + \varpi_2\right)\right)}$

with $b_1 > \gamma_{thf}\left(\kappa_t^2 + \varpi_2\right)$, $\tau_2 = \dfrac{\gamma_{thm} \vartheta_2}{\rho_r \left(b_2 - \gamma_{thm}\left(b_1 + \kappa_t^2 + \varpi_2\right)\right)}$ with $b_2 > \gamma_{thm}\left(b_1 + \kappa_t^2 + \varpi_2\right)$,

$\lambda_1 = 1 / \left(\rho_u \hat{\delta}_2^2 \left(a_2 + \kappa_r^2\right)\right)$, $\lambda_2 = 1 / \left(\rho_u \hat{\delta}_3^2 \left(\varpi_1 a_3 + \kappa_r^2\right)\right)$ and $\lambda_3 = 1 / \left(\rho_u \hat{\delta}_4^2 \left(\varpi_1 a_4 + \kappa_r^2\right)\right)$.

Proof: See Appendix A. ∎

Corollary 1. For the ideal cases $\left(\delta_{e_i}^2 = 0, \kappa_l = 0\right)$, the analytical expression for the outage probability of U_1 is expressed as

$$P_{U_1}^{id,out} = 1 - e^{-\frac{\gamma_{thf}}{\xi_1} - \frac{\tau_0'}{\delta_3^2}} \prod_{i=4}^{6} \lambda_i \left(\frac{\Psi_1 \xi_1}{\xi_1 \lambda_4 + \gamma_{thf}} - \frac{\Psi_2 \xi_1}{\xi_1 \lambda_5 + \gamma_{thf}} + \frac{\Psi_3 \xi_1}{\xi_1 \lambda_6 + \gamma_{thf}} \right) \tag{12}$$

where $\Psi_1 = \left(\lambda_5 - \lambda_4\right)^{-1}\left(\lambda_6 - \lambda_4\right)^{-1}$, $\Psi_2 = \left(\lambda_6 - \lambda_5\right)^{-1}\left(\lambda_5 - \lambda_4\right)^{-1}$, $\Psi_3 = \left(\lambda_6 - \lambda_4\right)^{-1}\left(\lambda_6 - \lambda_5\right)^{-1}$, $\tau_0' = \max\left(\tau_2', \tau_1'\right)$, $\tau_1' = \dfrac{\gamma_{thf}}{\rho_r \left(b_1 - \gamma_{thf} \varpi_2\right)}$ with $b_1 > \gamma_{thf} \varpi_2$ and $\tau_2' = \dfrac{\gamma_{thm}}{\rho_r \left(b_2 - \gamma_{thm}\left(b_1 + \varpi_2\right)\right)}$

with $b_2 > \gamma_{thm}\left(b_1 + \varpi_2\right)$, $\xi_1 = \rho_u a_1 \delta_1^2$, $\lambda_4 = 1 / \left(\rho_u a_2 \delta_2^2\right)$, $\lambda_5 = 1 / \left(\varpi_1 \rho_u a_3 \delta_3^2\right)$ and $\lambda_6 = 1 / \left(\varpi_1 \rho_u a_4 \delta_4^2\right)$.

Proof: See Appendix B.   ∎

2) Outage probability for U_2

The outage events of U_2 include four conditions as follows: *i*) The information x_1 cannot be decoded correctly by relay. *ii*) The relay cannot decode x_2, while the relay can first decode x_1, successfully. *iii*) U_3 cannot decode x_2 correctly. *iv*) x_2 cannot be decoded by U_4 successfully. Therefore, the outage probability of U_2 can be expressed as

$$P_{U_2}^{out} = 1 - \Pr\left(\gamma_{R \to x_2} > \gamma_{thm}, \gamma_{R \to x_1} > \gamma_{thf}\right) \Pr\left(\gamma_{u_3 \to x_2} > \gamma_{thm}\right) \Pr\left(\gamma_{u_4 \to x_2} > \gamma_{thm}\right) \tag{13}$$

Then, the outage probability of U_2 for the TWR-NOMA system with RHIs and CEEs is provided in the following theorem.

Theorem 2. For the non-ideal cases $\left(\delta_{e_i}^2 \neq 0, \kappa_l \neq 0\right)$, the exact analytical expression of U_2 in terms of outage probability is expressed as

$$P_{U_2}^{ni,out} = 1 - e^{-\left(\frac{\theta_2 \vartheta_1}{\hat{\delta}_2^2} + \frac{\theta_1 \vartheta_1}{\hat{\delta}_1^2} + \frac{\tau_2}{\hat{\delta}_3^2} + \frac{\tau_3}{\hat{\delta}_4^2}\right)} \frac{\hat{\delta}_2^2 \hat{\delta}_1^2 \lambda_1' \lambda_2'}{\left(\theta_2 \kappa_r^2 \rho_u \hat{\delta}_1^2 + \hat{\delta}_2^2\right)\left(\theta_1 \rho_u \hat{\delta}_2^2 \left(a_2 + \kappa_r^2\right) + \hat{\delta}_1^2\right)\left(\lambda_2' - \lambda_1'\right)}$$

$$\times \left(\frac{\hat{\delta}_1^2 \hat{\delta}_2^2}{\theta_2 \hat{\delta}_1^2 + \theta_1 \hat{\delta}_2^2 + \lambda_1' \hat{\delta}_1^2 \hat{\delta}_2^2} - \frac{\hat{\delta}_1^2 \hat{\delta}_2^2}{\theta_2 \hat{\delta}_1^2 + \theta_1 \hat{\delta}_2^2 + \lambda_2' \hat{\delta}_1^2 \hat{\delta}_2^2}\right) \tag{14}$$

where $\lambda_1' = 1 / \left(\rho_u \hat{\delta}_3^2 \left(\varpi_1 a_3 + \kappa_r^2\right)\right)$ and $\lambda_2' = 1 / \left(\rho_u \hat{\delta}_4^2 \left(\varpi_1 a_4 + \kappa_r^2\right)\right)$. $\theta_2 = \dfrac{\gamma_{thm}}{\rho_u \left(a_2 - \gamma_{thm} \kappa_r^2\right)}$

with $a_2 > \gamma_{thm} \kappa_r^2$. $\tau_3 = \dfrac{\gamma_{thm} \vartheta_3}{\rho_r \left(b_2 - \gamma_{thm} \left(b_1 + \kappa_t^2 + \varpi_2\right)\right)}$ with $b_2 > \gamma_{thm} \left(b_1 + \kappa_t^2 + \varpi_2\right)$.

Proof: See Appendix C.   ∎

Corollary 2. For the ideal cases $\left(\delta_{e_i}^2 = 0, \kappa_l = 0\right)$, the analytical expression for the outage probability with the ideal case of U_2 is expressed as

$$P_{U_2}^{id,out} = 1 - e^{-\left(\frac{\gamma_{thm} \beta_t}{\rho_u a_2} + \frac{\gamma_{thf}}{\rho_u a_1 \delta_1^2} + \frac{\tau_2'}{\delta_3^2} + \frac{\tau_2'}{\delta_4^2}\right)} \frac{\lambda_5 \lambda_6}{\beta_t \delta_2^2 \left(\lambda_6 - \lambda_5\right)} \sum_{k=5}^{6} \frac{(-1)^{k+1} \rho_u a_2}{\beta_t \gamma_{thm} + \lambda_k \rho_u a_2} \tag{15}$$

where $\tau_2' = \dfrac{\gamma_{thm}}{\rho_r \left(b_2 - \gamma_{thm} \left(b_1 + \varpi_2\right)\right)}$ with $b_2 > \gamma_{thm} \left(b_1 + \varpi_2\right)$ and $\beta_t = \dfrac{\gamma_{thf} a_2}{a_1 \delta_1^2} + \dfrac{1}{\delta_2^2}$.

$Y' = Y_5 + Y_6$ with $\lambda_5 = 1 / \left(\varpi_1 \rho_u a_3 \delta_3^2\right)$, $\lambda_6 = 1 / \left(\varpi_1 \rho_u a_4 \delta_4^2\right)$.

Proof: See Appendix D.   ∎

3.2 Asymptotic Outage Probability

To gain more insights, the asymptotic outage behavior is studied in the high SNR region. For the TWR-NOMA system, $\rho_u = \varepsilon \rho_r \to \infty$ and $\varepsilon > 0$. The asymptotic SINR of (3) and (4) can be approximately expressed as

5378

Tian et al.: Performance Analysis of Two-Way Relay NOMA Systems
with Hardware Impair-ments and Channel Estimation Errors

$$\overline{\gamma}_{R \to x_1} = \frac{\left|\hat{h}_1\right|^2 a_1}{\kappa_r^2 \left|\hat{h}_1\right|^2 + \left|\hat{h}_2\right|^2 \left(a_2 + \kappa_r^2\right) + \left|\hat{h}_3\right|^2 \left(\varpi_1 a_3 + \kappa_r^2\right) + \left|\hat{h}_4\right|^2 \left(\varpi_1 a_4 + \kappa_r^2\right) + \overline{\vartheta}_1} \tag{16}$$

$$\overline{\gamma}_{R \to x_2} = \frac{\left|\hat{h}_2\right|^2 a_2}{\kappa_r^2 \left|\hat{h}_1\right|^2 + \kappa_r^2 \left|\hat{h}_2\right|^2 + \left|\hat{h}_3\right|^2 \left(\varpi_1 a_3 + \kappa_r^2\right) + \left|\hat{h}_4\right|^2 \left(\varpi_1 a_4 + \kappa_r^2\right) + \overline{\vartheta}_1} \tag{17}$$

where $\overline{\vartheta}_1 = a_1 \delta_{e_1}^2 + a_2 \delta_{e_2}^2 + \varpi_1 a_3 \delta_{e_3}^2 + \varpi_1 a_4 \delta_{e_4}^2 + k_r^2 \left(\delta_{e_1}^2 + \delta_{e_2}^2 + \delta_{e_3}^2 + \delta_{e_4}^2\right)$.

The asymptotic SINR of (7), (8) and (9) can be approximately expressed as

$$\overline{\gamma}_{U_3 \to x_2} = \frac{\left|\hat{h}_3\right|^2 b_2}{\left|\hat{h}_3\right|^2 b_1 + \left|\hat{h}_3\right|^2 \kappa_t^2 + \varpi_2 \left|\hat{h}_3\right|^2 + \overline{\vartheta}_2} \tag{18}$$

$$\overline{\gamma}_{U_3 \to x_1} = \frac{\left|\hat{h}_3\right|^2 b_1}{\left|\hat{h}_3\right|^2 \kappa_t^2 + \varpi_2 \left|\hat{h}_3\right|^2 + \overline{\vartheta}_2} \tag{19}$$

$$\overline{\gamma}_{U_4 \to x_2} = \frac{\left|\hat{h}_4\right|^2 b_2}{\left|\hat{h}_4\right|^2 b_1 + \left|\hat{h}_4\right|^2 \kappa_t^2 + \varpi_2 \left|\hat{h}_4\right|^2 + \overline{\vartheta}_3} \tag{20}$$

where $\overline{\vartheta}_2 = \delta_{e_3}^2 + \delta_{e_3}^2 \kappa_t^2 + \varpi_2 \delta_{e_3}^2$ and $\overline{\vartheta}_3 = \delta_{e_4}^2 + \delta_{e_4}^2 \kappa_t^2 + \varpi_2 \delta_{e_4}^2$.

Lemma 1. *For the non-ideal cases* $\left(\delta_{e_i}^2 \neq 0, \kappa_l \neq 0\right)$, *the asymptotic outage probability of* U_1 *and* U_2 *can be derived as following*

$$P_{U_1}^{ni,\infty} \approx 1 - e^{-\frac{\overline{\tau}_0}{\hat{\delta}_3^2} - \frac{\overline{\theta}_1 \overline{\vartheta}_1}{\hat{\delta}_1^2}} \prod_{i=1}^{3} \overline{\lambda}_i \left(\frac{\overline{\Phi}_1 \hat{\delta}_1^2}{\overline{\lambda}_1 \hat{\delta}_1^2 + \overline{\theta}_1} - \frac{\overline{\Phi}_2 \hat{\delta}_1^2}{\overline{\lambda}_2 \hat{\delta}_1^2 + \overline{\theta}_1} + \frac{\overline{\Phi}_3 \hat{\delta}_1^2}{\overline{\lambda}_3 \hat{\delta}_1^2 + \overline{\theta}_1}\right) \tag{21}$$

where $\overline{\Phi}_1 = \left(\overline{\lambda}_2 - \overline{\lambda}_1\right)^{-1} \left(\overline{\lambda}_3 - \overline{\lambda}_1\right)^{-1}$, $\overline{\Phi}_2 = \left(\overline{\lambda}_3 - \overline{\lambda}_2\right)^{-1} \left(\overline{\lambda}_2 - \overline{\lambda}_1\right)^{-1}$, $\overline{\Phi}_3 = \left(\overline{\lambda}_3 - \overline{\lambda}_1\right)^{-1} \left(\overline{\lambda}_3 - \overline{\lambda}_2\right)^{-1}$.

$\overline{\lambda}_1 = 1 / \left(\hat{\delta}_2^2 \left(a_2 + \kappa_r^2\right)\right)$, $\overline{\lambda}_2 = 1 / \left(\hat{\delta}_3^2 \left(\varpi_1 a_3 + \kappa_r^2\right)\right)$, $\overline{\lambda}_3 = 1 / \left(\hat{\delta}_4^2 \left(\varpi_1 a_4 + \kappa_r^2\right)\right)$. $\overline{\theta}_1 = \frac{\gamma_{thf}}{\left(a_1 - \gamma_{thf} \kappa_r^2\right)}$

with $a_1 > \gamma_{thf} \kappa_r^2$, $\overline{\tau}_0 = \max\left(\overline{\tau}_2, \overline{\tau}_1\right)$, $\overline{\tau}_1 = \frac{\gamma_{thf} \overline{\vartheta}_2}{\left(b_1 - \gamma_{thf} \left(\kappa_t^2 + \varpi_2\right)\right)}$ *with* $b_1 > \gamma_{thf} \left(\kappa_t^2 + \varpi_2\right)$ *and*

$\overline{\tau}_2 = \frac{\gamma_{thm} \overline{\vartheta}_2}{\left(b_2 - \gamma_{thm} \left(b_1 + \kappa_t^2 + \varpi_2\right)\right)}$ *with* $b_2 > \gamma_{thm} \left(b_1 + \kappa_t^2 + \varpi_2\right)$.

$$P_{U_2}^{ni,\infty} \approx 1 - e^{-\left(\frac{\theta_2 \overline{\vartheta}_1}{\hat{\delta}_2^2} + \frac{\theta_1 \overline{\vartheta}_1}{\hat{\delta}_1^2} + \frac{\overline{\tau}_2}{\hat{\delta}_3^2} + \frac{\overline{\tau}_3}{\hat{\delta}_4^2}\right)} \frac{\hat{\delta}_2^2 \hat{\delta}_1^2 \overline{\lambda}_1' \overline{\lambda}_2'}{\left(\theta_2 \kappa_r^2 \hat{\delta}_1^2 + \hat{\delta}_2^2\right)\left(\theta_1 \hat{\delta}_2^2 \left(a_2 + \kappa_r^2\right) + \hat{\delta}_1^2\right)\left(\overline{\lambda}_2' - \overline{\lambda}_1'\right)}$$

$$\times \left(\frac{\hat{\delta}_1^2 \hat{\delta}_2^2}{\overline{\theta}_2 \hat{\delta}_1^2 + \overline{\theta}_1 \hat{\delta}_2^2 + \overline{\lambda}_1' \hat{\delta}_1^2 \hat{\delta}_2^2} - \frac{\hat{\delta}_1^2 \hat{\delta}_2^2}{\overline{\theta}_2 \hat{\delta}_1^2 + \overline{\theta}_1 \hat{\delta}_2^2 + \overline{\lambda}_2' \hat{\delta}_1^2 \hat{\delta}_2^2}\right) \tag{22}$$

where $\bar{\lambda}_1' = 1 / \left(\hat{\delta}_3^2 \left(\varpi_1 a_3 + \kappa_r^2 \right) \right)$, $\bar{\lambda}_2' = 1 / \left(\hat{\delta}_4^2 \left(\varpi_1 a_4 + \kappa_r^2 \right) \right)$. $\bar{\theta}_2 = \dfrac{\gamma_{thm}}{a_2 - \gamma_{thm} \kappa_r^2}$ *with* $a_2 > \gamma_{thm} \kappa_r^2$.

$\bar{\tau}_3 = \dfrac{\gamma_{thm} \bar{\vartheta}_3}{b_2 - \gamma_{thm} \left(b_1 + \kappa_t^2 + \varpi_2 \right)}$ *with* $b_2 > \gamma_{thm} \left(b_1 + \kappa_t^2 + \varpi_2 \right)$.

Lemma 2. *Based on the derived results of (12) and (15), when* $\rho_u = \varepsilon \rho_r \to \infty$*, and* $\varepsilon > 0$*, using* $e^{-x} = 1 - x$ *and L'Hospital's rule, the ideal cases* $\left(\delta_{e_i}^2 = 0, \kappa_l = 0 \right)$ *of the outage probability of* U_1 *and* U_2 *can be approximated as follows*

$$P_{U_1}^{id,\infty} \approx 1 - \prod_{i=4}^{6} \bar{\lambda}_i \left(\frac{\bar{\Psi}_1 a_1 \delta_1^2}{a_1 \delta_1^2 \bar{\lambda}_4 + \gamma_{thf}} - \frac{\bar{\Psi}_2 a_1 \delta_1^2}{a_1 \delta_1^2 \bar{\lambda}_5 + \gamma_{thf}} + \frac{\bar{\Psi}_3 a_1 \delta_1^2}{a_1 \delta_1^2 \bar{\lambda}_6 + \gamma_{thf}} \right) \tag{23}$$

where $\bar{\Psi}_1 = \left(\bar{\lambda}_5 - \bar{\lambda}_4 \right)^{-1} \left(\bar{\lambda}_6 - \bar{\lambda}_4 \right)^{-1}$, $\bar{\Psi}_2 = \left(\bar{\lambda}_6 - \bar{\lambda}_5 \right)^{-1} \left(\bar{\lambda}_5 - \bar{\lambda}_4 \right)^{-1}$, $\bar{\Psi}_3 = \left(\bar{\lambda}_6 - \bar{\lambda}_4 \right)^{-1} \left(\bar{\lambda}_6 - \bar{\lambda}_5 \right)^{-1}$. $\bar{\lambda}_4 = 1 / \left(a_2 \delta_2^2 \right)$, $\bar{\lambda}_5 = 1 / \left(\varpi_1 a_3 \delta_3^2 \right)$ *and* $\bar{\lambda}_6 = 1 / \left(\varpi_1 a_4 \delta_4^2 \right)$.

$$P_{U_2}^{id,\infty} \approx 1 - \frac{\bar{\lambda}_5 \bar{\lambda}_6}{\beta_t \delta_2^2 \left(\bar{\lambda}_6 - \bar{\lambda}_5 \right)} \sum_{k=5}^{6} \frac{(-1)^{k+1} a_2}{\beta_t \gamma_{thm} + \bar{\lambda}_k a_2} \tag{24}$$

where $\beta_t = \dfrac{\gamma_{thf} a_2}{a_1 \delta_1^2} + \dfrac{1}{\delta_2^2}$.

3) Diversity Orders

In this subsection, the diversity order is analyzed, which is defined as [34]

$$d = - \lim_{\rho \to \infty} \frac{\log \left(P_{U_n}^{\infty} (\rho) \right)}{\log \rho} \tag{25}$$

where $P_{U_n}^{\infty}$ denotes the asymptotic outage probability of U_n, $n \in \{1, 2\}$.

By using the definition in (25), the diversity orders for the non-ideal conditions $\left(\delta_{e_i}^2 \neq 0, \kappa_l \neq 0 \right)$ of both U_1 and U_2 are obtained as

$$d_1^{ni} = - \lim_{\rho \to \infty} \frac{\log \left(P_{U_1}^{ni,\infty} (\rho) \right)}{\log \rho} = 0 \tag{26}$$

$$d_2^{ni} = - \lim_{\rho \to \infty} \frac{\log \left(P_{U_2}^{ni,\infty} (\rho) \right)}{\log \rho} = 0 \tag{27}$$

The diversity orders for the ideal conditions $\left(\delta_{e_i}^2 = 0, \kappa_l = 0 \right)$ of both U_1 and U_2 are derived as

$$d_1^{id} = - \lim_{\rho \to \infty} \frac{\log \left(P_{U_1}^{id,\infty} (\rho) \right)}{\log \rho} = 0 \tag{28}$$

$$d_2^{id} = - \lim_{\rho \to \infty} \frac{\log \left(P_{U_2}^{id,\infty} (\rho) \right)}{\log \rho} = 0 \tag{29}$$

Remark: As can be observed from (21)-(24), there exists error floors for both the ideal and non-ideal conditions due to the intra-group interference. In addition, RHIs and CEEs deteriorate the outage probability since they can be recognized extra interference. As can also be seen in (26)-(29), the diversity orders for the ideal and non-ideal conditions are both zero due to the fixed outage probabilities at high SNRs. This means that TWR-NOMA can not obtain diversity gains.

4. Numerical Results and Discussions

In this section, some numerical results are provided to verify the accuracy of the theoretical analysis. We provide numerical illustration of our analytical results through Monte Carlo Simulations. Unless otherwise specified, the parameter values are provided in the Table 1. For convenience, we assume $\delta_e^2 = \delta_{e_1}^2 = \delta_{e_2}^2 = \delta_{e_3}^2 = \delta_{e_4}^2$, $\kappa = \kappa_r = \kappa_t$.

Table 1. Table of simulation parameters for numerical results

| Simulation parameters	Values
Monte Carlo simulations repeated	10^5 iterations
Power allocation coefficients of NOMA in the first phase	$a_1 = a_3 = 0.75$, $a_2 = a_4 = 0.25$
Power allocation coefficients of NOMA in the second phase	$b_1 = b_3 = 0.25$, $b_2 = b_4 = 0.75$
Average gain of estimated channel for $\hat{h}_1$, $\hat{h}_2$	$\hat{\delta}_1^2 = d_1^{-\alpha}$, $\hat{\delta}_2^2 = d_2^{-\alpha}$
The distance between R and U_1 or U_3	$d_1 = 2m$
The distance between R and U_2 or U_4	$d_2 = 4m$
Pass loss exponent	$\alpha = 4$
Targeted data rates	$R_f = 0.1$ BPCU and $R_m = 0.01$ BPCU
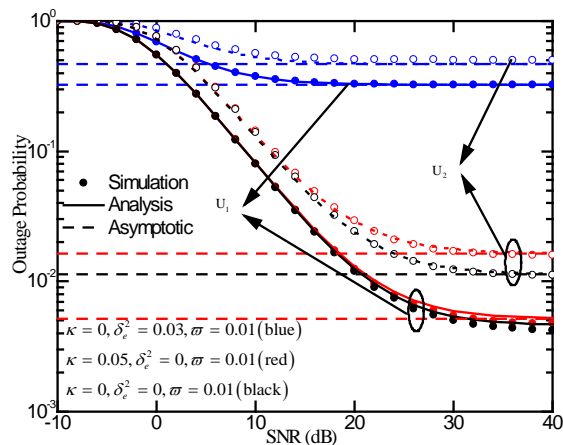
Fig. 2. Outage probability versus the transmit SNR.

Fig. 2 plots the outage probabilities of the two users versus transmit SNR for different values of κ and δ_e^2. We consider three cases in this simulation. 1) $\kappa = 0$, $\delta_e^2 = 0.03$; 2) $\kappa = 0.05$, $\delta_e^2 = 0$; 3) $\kappa = 0$, $\delta_e^2 = 0$. The curves represent the exact and asymptotic analytical of outage probability for U_1 and U_2 of ideal and non-ideal conditions in (11), (12), (14), (15) and (21), (22), (23), (24), respectively. It is clear that analytical curves are in good agreement with Monte Carlo simulations. It can be seen from this figure that the outage performance of the system with RHIs or CEEs is worse than that of the system without RHIs and CEEs for both U_1 and U_2, which means that RHIs and CEEs have deleterious effects on the system outage performance. Moreover, it is readily noticed from **Fig. 2** that for the third case, there are error floors for U_1 and U_2. The reason can be explained that the intra-group IS result in zero diversity orders. This conclusion is confirmed by (28) and (29).
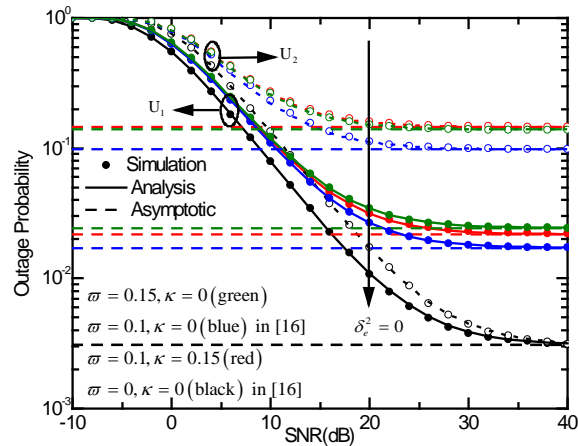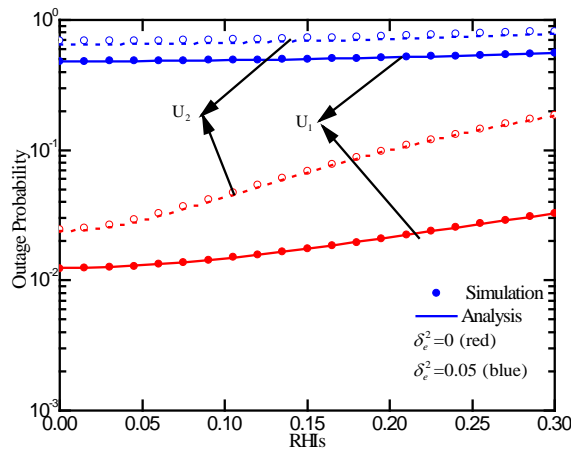

Fig. 3. Outage probability versus the transmit SNR.

Fig. 3 plots the outage performance versus SNR with different levels of inter-group IS from $\varpi = \{0, 0.1, 0.15\}$. For the purpose of comparison, the results of [16] have been provided. It can be seen that with the improvement of inter-group IS coefficient, the outage performance decreases obviously. We can conclude that the existence of the inter-group IS makes the outage performance worse. In addition, for the case $(\varpi = 0)$ and $(\varpi = 0.1)$, it still have the error floors caused by the intra-group IS, which is consistent with the results of **[16]**. We can observe that RHIs has a negative effect on the outage performance by comparing the red curves with the blue curves.
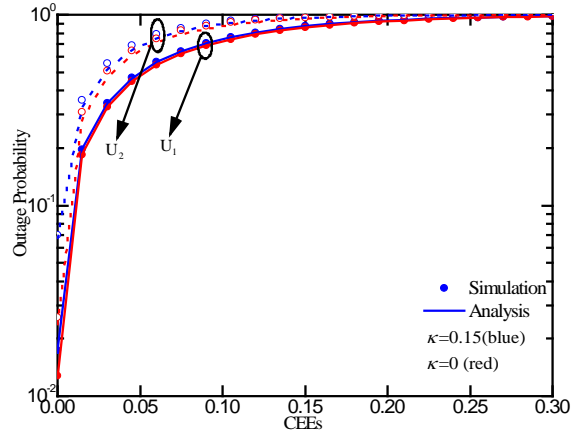
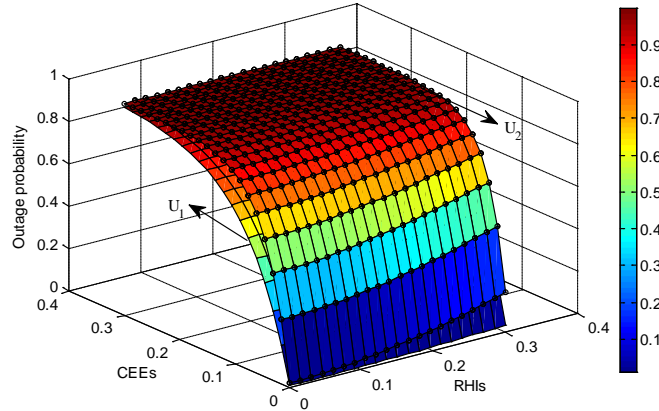**Fig. 4.** Outage probability versus the CEEs.

Fig. 4 plots the outage performance of the TWR-NOMA system versus CEEs for different RHIs parameters $\kappa = \{0, 0.15\}$. As observed from **Fig. 4**, the outage probabilities of the TWR-NOMA network for the two users increase as CEEs grow large. This happens because the CEEs act as interference for the desired signal, which reduces the system performance. Moreover, the growth of U_1 is larger than that of U_2, which means that CEEs have more serious effect on the outage probabilities of the near users than the far users for this system.

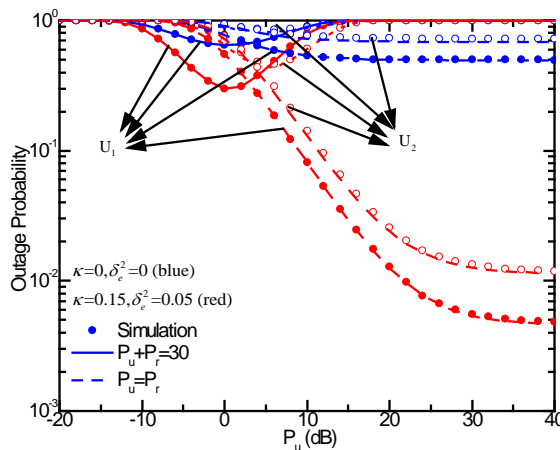**Fig. 5.** Outage probability versus the RHIs at the relay node.

Fig. 5 illustrates the impact of the RHIs at the relay node on the outage performance of the TWR-NOMA systems. These curves represent two cases: ideal case $\left(\delta_e^2 = 0\right)$ and non-ideal case $\left(\delta_e^2 = 0.05\right)$. In addition, we assume a fixed transmit SNR (20dB) in this simulation. It can be observed that the outage performance becomes worse as the RHIs increase in both two

cases. Moreover, when the RHIs is equal to zero $(\kappa = 0)$, the outage probabilities of this two cases have different values, due to the CEEs existence in the non-ideal case.

Fig. 6. Outage probability versus the RHIs and CEEs.

Fig. 6 illustrates the impact of the RHIs and the CEEs at the relay node on the outage performance of the TWR-NOMA systems. We use the change of color to reflect the outage performance affected. There is a chromaticity bar on the right side of the graph. As the color changes from dark to light indicates that the performance of system outage becomes degrades. There are two layers of grid in this figure, the lower one denotes the performance of U_1 and the other layer denotes the performance of U_2. This means that the performance of U_1 is better than that of U_2. It is apparent to see from the **Fig. 6** that as RHIs increase, the color changes from dark blue to light blue, and as the CEEs increase, the color clearly changes from dark to light, which means the outage probability becomes worse, respectively.

Fig. 7. Outage probability versus P_u

Fig. 7 depicts the impact of P_u on the outage performance. In this simulation, we consider two cases: 1) $P_u = -20:40$ dB and $P_u + P_r = 30dB$; 2) $P_u = -20:40$ dB and $P_u = P_r$. For the first case, we can clearly see that there exist optimal allocation powers (about 0dB for U_1 and 6dB for U_2) for P_u of U_1 and U_2. This happens because the performance gain caused by increasing the power of users (P_u) is larger than the performance loss caused by reducing the power of relay (P_r). For the second case, we can also see that the outage probabilities for the two users always decrease as the power of users and relay increasing.

5. Conclusion

This paper investigated the performance of TWR-NOMA networks with RHIs and CEEs, in which two groups of users exchange information with the aid of a DF relay. The closed-form expressions for exact outage probability of two group users were derived and the asymptotic behavior was discussed. Based on the derived analytical results, we further evaluated the diversity orders achieved by the users. Results revealed that CEEs have more deleterious effects on the outage probabilities of the near users than the far users. Furthermore, it was shown that the TWR-NOMA networks with inter-group IS, intra-group IS, RHIs or CEEs cause error floors.

APPENDIX A

PROOF OF THEOREM 1

It is worth noting that for the convenience of calculation, we assume $X_i = |h_i|^2$, $\hat{X}_i = |\hat{h}_i|^2$ with $i \in \{1, 2, 3, 4\}$. Substituting (3), (7) and (8) into (10), the outage probability of U_1 is given by

$$
\begin{aligned}
\mathrm{P}_{U_1}^{ni,out} &= 1 - \Pr\left(\gamma_{R \to x_1} > \gamma_{thf}\right)\Pr\left(\gamma_{U_3 \to x_2} > \gamma_{thm}, \gamma_{U_3 \to x_1} > \gamma_{thf}\right) \\
&= 1 - f_1 f_2
\end{aligned}
\tag{A.1}
$$

$$
f_1 = \Pr\left(\frac{\rho_u |\hat{h}_1|^2 a_1}{\rho_u |\hat{h}_2|^2 a_2 + \sum_{k=1}^{4} \rho_u |\hat{h}_k|^2 \kappa_r^2 + \sum_{j=3}^{4} \rho_u |\hat{h}_j|^2 \varpi_1 a_j + \vartheta_1} > \gamma_{thf}\right),
\tag{A.2}
$$

$$
f_2 = \Pr\left(\frac{\rho_r |\hat{h}_3|^2 b_2}{\rho_r |\hat{h}_3|^2 b_1 + \rho_r |\hat{h}_3|^2 \kappa_t^2 + \varpi_2 \rho_r |\hat{h}_3|^2 + \vartheta_2} > \gamma_{thm},\right.
$$

$$
\left.\frac{\rho_r |\hat{h}_3|^2 b_1}{\rho_r |\hat{h}_3|^2 \kappa_t^2 + \varpi_2 \rho_r |\hat{h}_3|^2 + \vartheta_2} > \gamma_{thf}\right),
\tag{A.3}
$$

For calculating the probability of f_1 in (A.2), we set $z = z_1 + z_2 + z_3$ with $z_1 = \rho_u \left| \hat{h}_2 \right|^2 \left(a_2 + \kappa_r^2 \right)$, $z_2 = \rho_u \left| \hat{h}_3 \right|^2 \left(\varpi_1 a_3 + \kappa_r^2 \right)$, and $z_3 = \rho_u \left| \hat{h}_4 \right|^2 \left(\varpi_1 a_4 + \kappa_r^2 \right)$. As we wrote earlier, $\left| \hat{h}_i \right|^2$ follow the exponential distribution with the means $\hat{\delta}_i^2$, $i \in \{1, 2, 3, 4\}$. In addition, z_1, z_2, and z_3 are also independent exponentially distributed random variables with means $\lambda_1 = 1 / \left(\rho_u \hat{\delta}_2^2 \left(a_2 + \kappa_r^2 \right) \right)$, $\lambda_2 = 1 / \left(\rho_u \hat{\delta}_3^2 \left(\varpi_1 a_3 + \kappa_r^2 \right) \right)$, and $\lambda_3 = 1 / \left(\rho_u \hat{\delta}_4^2 \left(\varpi_1 a_4 + \kappa_r^2 \right) \right)$, respectively. As shown in the [35], for the independent non-identical distributed fading scenario, the PDF of z is given by

$$f_Z(z) = \prod_{t=1}^{3} \lambda_t \left(\Phi_1 e^{-\lambda_1 z} - \Phi_2 e^{-\lambda_2 z} + \Phi_3 e^{-\lambda_3 z} \right), \tag{A.4}$$

where $\Phi_1 = \left(\lambda_2 - \lambda_1 \right)^{-1} \left(\lambda_3 - \lambda_1 \right)^{-1}$, $\Phi_2 = \left(\lambda_3 - \lambda_2 \right)^{-1} \left(\lambda_2 - \lambda_1 \right)^{-1}$, $\Phi_3 = \left(\lambda_3 - \lambda_1 \right)^{-1} \left(\lambda_3 - \lambda_2 \right)^{-1}$.

According to the above explanations, f_1 is expressed as follows

$$\begin{aligned} f_1 &= \Pr\left(\hat{X}_1 > \theta_1 \left(z + \vartheta_1 \right) \right) \\ &= e^{-\frac{\theta_1 \vartheta_1}{\hat{\delta}_1^2}} \prod_{i=1}^{3} \lambda_i \left(\frac{\Phi_1 \hat{\delta}_1^2}{\lambda_1 \hat{\delta}_1^2 + \theta_1} - \frac{\Phi_2 \hat{\delta}_1^2}{\lambda_2 \hat{\delta}_1^2 + \theta_1} + \frac{\Phi_3 \hat{\delta}_1^2}{\lambda_3 \hat{\delta}_1^2 + \theta_1} \right), \end{aligned} \tag{A.5}$$

where $\theta_1 = \dfrac{\gamma_{thf}}{\rho_u \left(a_1 - \gamma_{thf} \kappa_r^2 \right)}$, with $a_1 > \gamma_{thf} \kappa_r^2$.

f_2 can be further calculated as follows

$$\begin{aligned} f_2 &= \Pr\left(\hat{X}_3 > \tau_2, \hat{X}_3 > \tau_1 \right) \\ &= \Pr\left(\hat{X}_3 > \max(\tau_2, \tau_1) = \tau_0 \right) \\ &= e^{-\frac{\tau_0}{\hat{\delta}_3^2}}, \end{aligned} \tag{A.6}$$

where $\tau_0 = \max(\tau_2, \tau_1)$, $\tau_2 = \dfrac{\gamma_{thm} \vartheta_2}{\rho_r \left(b_2 - \gamma_{thm} \left(b_1 + \kappa_t^2 + \varpi_2 \right) \right)}$ with $b_2 > \gamma_{thm} \left(b_1 + \kappa_t^2 + \varpi_2 \right)$ and

$\tau_1 = \dfrac{\gamma_{thf} \vartheta_2}{\rho_r \left(b_1 - \gamma_{thf} \left(\kappa_t^2 + \varpi_2 \right) \right)}$ with $b_1 > \gamma_{thf} \left(\kappa_t^2 + \varpi_2 \right)$.

Substituting (A.5), (A.6) into (A.1), (11) can be obtained.
The proof is completed.

APPENDIX B

PROOF OF COROLLARY 1

The outage probability of U_1 for the ideal cases can be expressed as

5386

Tian et al.: Performance Analysis of Two-Way Relay NOMA Systems
with Hardware Impair-ments and Channel Estimation Errors

$$P_{U_1}^{id,out} = 1 - \Pr\left(\gamma_{R \to x_1} > \gamma_{thf}\right) \Pr\left(\gamma_{U_3 \to x_2} > \gamma_{thm}, \gamma_{U_3 \to x_1} > \gamma_{thf}\right)$$

$$= 1 - \Pr\left(\frac{\rho_u X_1 a_1}{\rho_u X_2 a_2 + \varpi_1 \rho_u X_3 a_3 + \varpi_1 \rho_u X_4 a_4 + 1} > \gamma_{thf}\right)$$

$$\times \Pr\left(\frac{\rho_r X_3 b_2}{\rho_r X_3 \left(b_1 + \varpi_2\right) + 1} > \gamma_{thm}, \frac{\rho_r X_3 b_1}{\rho_r X_3 \varpi_2 + 1} > \gamma_{thf}\right) \qquad \text{(B.1)}$$

$$= 1 - \Pr\left(X_1 > \frac{\gamma_{thf}}{\rho_u a_1}\left(Y + 1\right)\right) \Pr\left(X_3 > \tau_0' = \max\left(\tau_2', \tau_1'\right)\right)$$

$$= 1 - f_1' f_2',$$

where $Y = Y_4 + Y_5 + Y$, with $Y_4 = \rho_u a_2 X_2$, $Y_5 = \varpi_1 \rho_u a_3 X_3$, $Y_6 = \varpi_1 \rho_u a_4 X_4$. As we wrote earlier Y_4 , Y_5 and Y_6 are independent exponentially distributed random variables with means $\lambda_4 = 1/\left(\rho_u a_2 \delta_2^2\right)$, $\lambda_5 = 1/\left(\varpi_1 \rho_u a_3 \delta_3^2\right)$, and $\lambda_6 = 1/\left(\varpi_1 \rho_u a_4 \delta_4^2\right)$.

f_1' can be further expressed as follows

$$f_1' = \Pr\left(X_1 > \frac{\gamma_{thf}}{\rho_u a_1}\left(Y + 1\right)\right)$$

$$= e^{-\frac{\gamma_{thf}}{\xi_1}} \prod_{i=1}^{3} \lambda_i \left(\frac{\Psi_1 \xi_1}{\xi_1 \lambda_4 + \gamma_{thf}} - \frac{\Psi_2 \xi_1}{\xi_1 \lambda_5 + \gamma_{thf}} + \frac{\Psi_3 \xi_1}{\xi_1 \lambda_6 + \gamma_{thf}}\right), \qquad \text{(B.2)}$$

where $\Psi_1 = \left(\lambda_5 - \lambda_4\right)^{-1}\left(\lambda_6 - \lambda_4\right)^{-1}$, $\Psi_2 = \left(\lambda_6 - \lambda_5\right)^{-1}\left(\lambda_5 - \lambda_4\right)^{-1}$, $\Psi_3 = \left(\lambda_6 - \lambda_4\right)^{-1}\left(\lambda_6 - \lambda_5\right)^{-1}$. $\xi_1 = \rho_u a_1 \delta_1^2$.

f_2' can be easily calculated as follows

$$f_2' = \Pr\left(X_3 > \tau_0'\right) = e^{-\frac{\tau_0'}{\delta_3^2}}. \qquad \text{(B.3)}$$

where $\tau_0' = \max\left(\tau_2', \tau_1'\right)$, $\tau_1' = \dfrac{\gamma_{thf}}{\rho_r\left(b_1 - \gamma_{thf}\varpi_2\right)}$ with $b_1 > \gamma_{thf}\varpi_2$, $\tau_2' = \dfrac{\gamma_{thm}}{\rho_r\left(b_2 - \gamma_{thm}\left(b_1 + \varpi_2\right)\right)}$

with $b_2 > \gamma_{thm}\left(b_1 + \varpi_2\right)$.

Combining (B.2), (B.3) into (B.1), we can obtain (12).

The proof is completed.

APPENDIX C

PROOF OF THEOREM 2

The outage probability of U_2 can be expressed as

$$P_{U_2}^{ni,out} = 1 - \Pr\left(\gamma_{R \to x_2} > \gamma_{thm}, \gamma_{R \to x_1} > \gamma_{thf}\right) \Pr\left(\gamma_{u_3 \to x_2} > \gamma_{thm}\right) \Pr\left(\gamma_{u_4 \to x_2} > \gamma_{thm}\right)$$

$$= 1 - f_3 f_4 f_5 \qquad \text{(C.1)}$$

Substituting (3), (4) into (C.1), f_3 can be further given by

$$f_3 = \Pr\left(\gamma_{R \to x_2} > \gamma_{thm}, \gamma_{R \to x_1} > \gamma_{thf}\right)$$

$$= \Pr\left(\frac{\rho_u \left|\hat{h}_2\right|^2 a_2}{\sum_{k=1}^{4} \rho_u \left|\hat{h}_k\right|^2 \kappa_r^2 + \sum_{j=3}^{4} \rho_u \left|\hat{h}_j\right|^2 \varpi_1 a_j + \vartheta_1} > \gamma_{thm}, \right.$$

$$\left. \frac{\rho_u \left|\hat{h}_1\right|^2 a_1}{\rho_u \left|\hat{h}_2\right|^2 a_2 + \sum_{k=1}^{4} \rho_u \left|\hat{h}_k\right|^2 \kappa_r^2 + \sum_{j=3}^{4} \rho_u \left|\hat{h}_j\right|^2 \varpi_1 a_j + \vartheta_1} > \gamma_{thf} \right) \quad \text{(C.2)}$$

$$= \Pr\left(\hat{X}_2 > \theta_2 \left(\kappa_r^2 \rho_u \hat{X}_1 + z' + \vartheta_1 \right), \hat{X}_1 > \theta_1 \left(\rho_u \left(a_2 + \kappa_r^2 \right) \hat{X}_2 + z' + \vartheta_1 \right) \right)$$

$$= e^{-\left(\frac{\theta_2 \vartheta_1}{\hat{\delta}_2^2} + \frac{\theta_1 \vartheta_1}{\hat{\delta}_1^2} \right)} \frac{\hat{\delta}_2^2 \hat{\delta}_1^2}{\left(\theta_2 k_r^2 \rho_u \hat{\delta}_1^2 + \hat{\delta}_2^2 \right)\left(\theta_1 \rho_u \hat{\delta}_2^2 \left(a_2 + k_r^2 \right) + \hat{\delta}_1^2 \right)} \int_0^\infty e^{-\left(\frac{\theta_2}{\hat{\delta}_2^2} + \frac{\theta_1}{\hat{\delta}_1^2} \right) z'} f\left(z'\right) dz'.$$

For calculating the probability of f_3 in (C.1), we assume $z' = z_1' + z_2'$, with $z_1' = \rho_u \left|\hat{h}_3\right|^2 \left(\varpi_1 a_3 + \kappa_r^2 \right)$, and $z_2' = \rho_u \left|\hat{h}_4\right|^2 \left(\varpi_1 a_4 + \kappa_r^2 \right)$. z_1' and z_2' are also independent exponentially distributed random variables with means $\lambda_1' = 1 / \left(\rho_u \hat{\delta}_3^2 \left(\varpi_1 a_3 + \kappa_r^2 \right) \right)$ and $\lambda_2' = 1 / \left(\rho_u \hat{\delta}_4^2 \left(\varpi_1 a_4 + \kappa_r^2 \right) \right)$, respectively. For the independent non-identical distributed fading scenario, the PDF of z' is given by

$$f_{z'}(z') = \prod_{t=1}^{2} \lambda_i' \left(\frac{e^{-\lambda_1 z'}}{\lambda_2' - \lambda_1'} - \frac{e^{-\lambda_2 z'}}{\lambda_2' - \lambda_1'} \right). \quad \text{(C.3)}$$

Substituting (C.3) into (C.2), f_3 can be further rewritten as

$$f_3 = e^{-\left(\frac{\theta_2 \vartheta_1}{\hat{\delta}_2^2} + \frac{\theta_1 \vartheta_1}{\hat{\delta}_1^2} \right)} \frac{\hat{\delta}_2^2 \hat{\delta}_1^2 \lambda_1' \lambda_2'}{\left(\theta_2 k_r^2 \rho_u \hat{\delta}_1^2 + \hat{\delta}_2^2 \right)\left(\theta_1 \rho_u \hat{\delta}_2^2 \left(a_2 + k_r^2 \right) + \hat{\delta}_1^2 \right)\left(\lambda_2' - \lambda_1' \right)}$$

$$\times \left(\frac{\hat{\delta}_1^2 \hat{\delta}_2^2}{\theta_2 \hat{\delta}_1^2 + \theta_1 \hat{\delta}_2^2 + \lambda_1' \hat{\delta}_1^2 \hat{\delta}_2^2} - \frac{\hat{\delta}_1^2 \hat{\delta}_2^2}{\theta_2 \hat{\delta}_1^2 + \theta_1 \hat{\delta}_2^2 + \lambda_2' \hat{\delta}_1^2 \hat{\delta}_2^2} \right). \quad \text{(C.4)}$$

Substituting (7), (9) into (C.1), f_4 and f_5 can be calculated as follows

$$f_4 = \Pr\left(\frac{\rho_r \left|\hat{h}_3\right|^2 b_2}{\rho_r \left|\hat{h}_3\right|^2 b_1 + \rho_r \left|\hat{h}_3\right|^2 k_t^2 + \varpi_2 \rho_r \left|\hat{h}_3\right|^2 + \vartheta_2} > \gamma_{thm} \right)$$

$$= \Pr\left(\hat{X}_3 > \tau_2 \right) \quad \text{(C.5)}$$

$$= e^{-\frac{\tau_2}{\hat{\delta}_3^2}}.$$

5388

Tian et al.: Performance Analysis of Two-Way Relay NOMA Systems
with Hardware Impair-ments and Channel Estimation Errors

$$f_5 = \Pr\left(\frac{\rho_r \left|\hat{h}_4\right|^2 b_2}{\rho_r \left|\hat{h}_4\right|^2 b_1 + \rho_r \left|\hat{h}_4\right|^2 \kappa_t^2 + \varpi_2 \rho_r \left|\hat{h}_4\right|^2 + \vartheta_3} > \gamma_{thm} \right)$$

$$= \Pr\left(\hat{X}_4 > \tau_3 \right) \tag{C.6}$$

$$= e^{-\frac{\tau_3}{\hat{\delta}_4^2}},$$

where $\tau_3 = \dfrac{\gamma_{thm}\vartheta_3}{\rho_r \left(b_2 - \gamma_{thm}\left(b_1 + \kappa_t^2 + \varpi_2 \right)\right)}$, with $b_2 > \gamma_{thm}\left(b_1 + \kappa_t^2 + \varpi_2 \right)$. Finally, (14) can be obtained by combing (C.4), (C.5), and (C.6).

The proof is completed.

APPENDIX D

PROOF OF COROLLARY 2

The outage probability of U_2 with ideal conditions can be expressed as

$$\mathrm{P}_{U_2}^{id,out} = 1 - \Pr\left(\gamma_{R\to x_2} > \gamma_{thm}, \gamma_{R\to x_1} > \gamma_{thf} \right)\Pr\left(\gamma_{U_3 \to x_2} > \gamma_{thm} \right)\Pr\left(\gamma_{U_4 \to x_2} > \gamma_{thm} \right)$$

$$= 1 - f_3' f_4' f_5' \tag{D.1}$$

f_3' can be further calculated as

$$f_3' = \Pr\left(\frac{\rho_u \left|h_2\right|^2 a_2}{\rho_u \left|h_3\right|^2 \varpi_1 a_3 + \rho_u \left|h_4\right|^2 \varpi_1 a_4 + 1} > \gamma_{thm}, \frac{\rho_u \left|h_1\right|^2 a_1}{\rho_u \left|h_2\right|^2 a_2 + \rho_u \left|h_3\right|^2 \varpi_1 a_3 + \rho_u \left|h_4\right|^2 \varpi_1 a_4 + 1} > \gamma_{thf} \right)$$

$$= \Pr\left(X_2 > \frac{\gamma_{thm}}{\rho_u a_2}\left(Y' + 1 \right), X_1 > \frac{\gamma_{thf}}{\rho_u a_1}\left(\rho_u a_2 X_2 + Y' + 1 \right) \right)$$

$$= \frac{1}{\beta_t \delta_2^2} e^{-\left(\frac{\gamma_{thm}\beta_t}{\rho_u a_2} + \frac{\gamma_{thf}}{\rho_u a_1 \delta_1^2} \right)} \int_0^\infty e^{-\frac{\gamma_{thm}\beta_t}{\rho_u a_2} Y'} f\left(Y' \right) dY'$$

$$= \frac{\lambda_5 \lambda_6}{\beta_t \delta_2^2 \left(\lambda_6 - \lambda_5 \right)} e^{-\left(\frac{\gamma_{thm}\beta_t}{\rho_u a_2} + \frac{\gamma_{thf}}{\rho_u a_1 \delta_1^2} \right)} \sum_{k=5}^{6} \frac{(-1)^{k+1} \rho_u a_2}{\beta_t \gamma_{thm} + \lambda_k \rho_u a_2},$$

$$\tag{D.2}$$

where $Y' = Y_5 + Y_6$. As we wrote earlier $Y_5 = \varpi_1 \rho_u a_3 X_3$, $Y_6 = \varpi_1 \rho_u a_4 X_4$. In addition, Y_5, Y_6 are independent exponentially distributed random variables with means $\lambda_5 = 1/\left(\varpi_1 \rho_u a_3 \delta_3^2 \right)$,

$\lambda_6 = 1/\left(\varpi_1 \rho_u a_4 \delta_4^2 \right)$, $\beta_t = \dfrac{\gamma_{thf} a_2}{a_1 \delta_1^2} + \dfrac{1}{\delta_2^2}$.

f_4' and f_5' are easily obtained as follows

$$f_4' = \Pr\left(\frac{\rho_r \left| h_3 \right|^2 b_2}{\rho_r \left| h_3 \right|^2 b_1 + \varpi_2 \rho_r \left| h_3 \right|^2 + 1} > \gamma_{thm} \right)$$

$$= \Pr\left(X_3 > \tau_2' \right) \tag{D.3}$$

$$= e^{-\frac{\tau_2'}{\delta_3^2}},$$

where $\tau_2' = \dfrac{\gamma_{thm}}{\rho_r \left(b_2 - \gamma_{thm} \left(b_1 + \varpi_2 \right) \right)}$ with $b_2 > \gamma_{thm} \left(b_1 + \varpi_2 \right)$.

$$f_5' = \Pr\left(\frac{\rho_r \left| h_4 \right|^2 b_2}{\rho_r \left| h_4 \right|^2 b_1 + \varpi_2 \rho_r \left| h_4 \right|^2 + 1} > \gamma_{thf} \right)$$

$$= \Pr\left(X_4 > \tau_2' \right) \tag{D.4}$$

$$= e^{-\frac{\tau_2'}{\delta_4^2}}.$$

Combining (D.2), (D.3) and (D.4) into (D.1), we can obtain (15).
The proof is completed.

References

[1] Z. Ding, F. Adachi, and H. V. Poor, "The Application of MIMO to Non-Orthogonal Multiple Access," *IEEE Trans. Wireless Commun.*, vol. 15, no. 1, pp. 537–552, Jan 2016. Article (CrossRef Link).

[2] J. Zeng, T. Lv, R. P. Liu, X. Su, M. Peng, C. Wang, and J. Mei, "Investigation on Evolving Single-Carrier NOMA Into Multi-Carrier NOMA in 5G," *IEEE Access*, vol. 6, pp. 48268–48288, 2018. Article (CrossRef Link).

[3] J. An, K. Yang, J. Wu, N. Ye, S. Guo and Z. Liao, "Achieving Sustainable Ultra-Dense Heterogeneous Networks for 5G," *IEEE Commun. Mag.*, vol. 55, no. 12, pp. 84-90, Dec. 2017. Article (CrossRef Link).

[4] S. M. R. Islam, N. Avazov, O. A. Dobre, and K. Kwak, "Power-Domain Non-Orthogonal Multiple Access (NOMA) in 5G Systems: Potentials and Challenges," *IEEE Communications Surveys Tutorials*, vol. 19, no. 2, pp. 721–742, Secondquarter 2017. Article (CrossRef Link).

[5] D. Duchemin, J. Gorce, and C. Goursaud, "Code Domain Non Orthogonal Multiple Access versus ALOHA: A simulation based study," in *Proc. of 2018 25th ICT*, pp. 445–450, Jun. 2018. Article (CrossRef Link).

[6] F. A. Rabee, K. Davaslioglu, and R. Gitlin, "The optimum received power levels of uplink non-orthogonal multiple access (NOMA) signals," in *Proc. of 2017 IEEE 18th WAMICON*, pp. 1–4, Apr. 2017. Article (CrossRef Link).

[7] B. Xia, J. Wang, K. Xiao, Y. Gao, Y. Yao, and S. Ma, "Outage Performance Analysis for the Advanced SIC Receiver in Wireless NOMA Systems," *IEEE Trans. Veh. Technol*, vol. 67, no. 7, pp. 6711–6715, Jul. 2018. Article (CrossRef Link).

[8] M. Sami, N. K. Noordin, M. Khabazian, F. Hashim, and S. Subramaniam, "A Survey and Taxonomy on Medium Access Control Strategies for Cooperative Communication in Wireless Networks: Research Issues and Challenges," *IEEE Commun. Surveys Tutorials*, vol. 18, no. 4, pp. 2493–2521, Fourthquarter 2016. Article (CrossRef Link).

[9] T. Cui, F. Gao, T. Ho, and A. Nallanathan, "Distributed Space–Time Coding for Two-Way Wireless Relay Networks," *IEEE Trans. Signal Process.*, vol. 57, no. 2, pp. 658–671, Feb. 2009. Article (CrossRef Link).

[10] K. Yang, N. Yang, C. Xing and J. Wu, "Relay Antenna Selection in MIMO Two-Way Relay Networks Over Nakagami-m Fading Channels," *IEEE Tran. Veh. Technol.,* vol. 63, no. 5, pp. 2349-2362, Jun 2014. Article (CrossRef Link).

[11] D. E. Simmons and J. P. Coon, "Two-Way OFDM-Based Nonlinear Amplify-and-Forward Relay Systems," *IEEE Trans. Vehicular Technology*, vol. 65, no. 5, pp. 3808–3812, May 2016. Article (CrossRef Link).

[12] Y. Qi and X. Wang, "Performance Optimization of Two-Way AF Relaying in Asymmetric Fading Channels," *KSII Trans. Internet & Information Systems*, vol. 8, no. 12, pp. 4432–4450, 2014. Article (CrossRef Link).

[13] X. Chen, L. Guo, C. Dong, J. Lin, X. Li and Charles C. Cavalcante, "Probabilistic Constrained Approach for Distributed Robust Beamforming Design in Cognitive Two-way Relay Networks," *KSII Trans. Internet & Information Systems*, vol. 12, no. 1, pp. 21–40, 2018. Article (CrossRef Link).

[14] G. Li, Y. Wang and P. Zhang, "Optimal Linear MMSE Beamforming for Two Way Multi-Antenna Relay Systems," *IEEE Commun. Lett.*, vol. 15, no. 5, pp. 533–535, 2011. Article (CrossRef Link).

[15] X. Li, Michail Matthaiou, Y. Liu, Hien Quoc Ngo and L. Li, "Multi-Pair Two-Way Massive MIMO Relaying with Hardware Impairments over Rician Fading Channels," in *Proc. of IEEE Globecom, Abu Dhabi*, Dec. 2018. Article (CrossRef Link).

[16] X. Yue, Y. Liu, S. Kang, A. Nallanathan, and Y. Chen, "Modeling and analysis of two-way relay non-orthogonal multiple access systems," *IEEE Trans. Commun.*, vol. 66, no. 9, pp. 3784–3796, Sep. 2018. Article (CrossRef Link).

[17] X. Wang, M. Jia, I. W. Ho, Q. Guo, and F. C. M. Lau, "Exploiting full-duplex two-way relay cooperative non-orthogonal multiple access," *IEEE Trans. Commun.*,vol. 67, no. 4, pp. 2716-2729, 2019. Article (CrossRef Link).

[18] B. Zheng, X. Wang, M. Wen, and F. Chen, "NOMA-Based Multi-Pair Two-Way Relay Networks With Rate Splitting and Group Decoding," *IEEE J. Selected Areas in Commun.*, vol. 35, no. 10, pp. 2328–2341, Oct. 2017. Article (CrossRef Link).

[19] B. Zheng, M. Wen, C. Wang, X. Wang, F. Chen, J. Tang, and F. Ji, "Secure NOMA Based Two-Way Relay Networks Using Artificial Noise and Full Duplex," *IEEE J. Selected Areas in Commun.*, vol. 36, no. 7, pp. 1426–1440, Jul. 2018. Article (CrossRef Link).

[20] E. Bjornson, M. Matthaiou, and M. Debbah, "A New Look at Dual-Hop Relaying: Performance Limits with Hardware Impairments," *IEEE Trans. Commun.*, vol. 61, no. 11, pp. 4512–4525, Nov. 2013. Article (CrossRef Link).

[21] T. T. Duy, T. Q. Duong, D. B. da Costa, V. N. Q. Bao, and M. Elkashlan, "Proactive Relay Selection With Joint Impact of Hardware Impairment and Co-Channel Interference," *IEEE Trans. Commun.*, vol. 63, no. 5, pp. 1594–1606, May 2015. Article (CrossRef Link).

[22] X. Li and J. Li and P. Takis Mathiopoulos and D. Zhang and L. Li and J. Jin, "Joint Impact of Hardware Impairments and Imperfect CSI on Cooperative SWIPT NOMA Multi-Relaying Systems," in *Proc. of IEEE/CIC International Conference on Commun. China (ICCC), Beijing, China,* 2018. Article (CrossRef Link).

[23] T. Schenk, *RF imperfections in high-rate wireless systems:impact and digital compensation*, Springer Verlag, New York, NY, USA, 2008. Article (CrossRef Link).

[24] X. Li and J. Li and J. Jin and L. Li, "Performance analysis of relaying systems over nakagami-m fading with transceiver hardware impairments," *Journal of Xidian University*, vol. 45, no. 3, pp. 135–140, Jun 2018. Article (CrossRef Link).

[25] C. Deng, X. Zhao, D. Zhang, X. Li, J. Li, Cavalcante, Charles, "Performance Analysis of NOMA-based Relaying Networks with Transceiver Hardware Impairments," *KSII Trans.Internet and Information Systems*, vol. 12, Feb. 2018. Article (CrossRef Link)

[26] A. Papazafeiropoulos, S. K. Sharma, T. Ratnarajah, and S. Chatzinotas, "Impact of residual additive transceiver hardware impairments on rayleigh-product mimo channels with linear receivers: Exact and asymptotic analyses," *IEEE Trans. Commun.*, vol. 66, no. 1, pp. 105–118, Jan 2018. Article (CrossRef Link).

[27] X. Li and M. Huang and X. Tian and H. Guo and J. Jin and C. Zhang, "Impact of Hardware Impairments on Large-scale MIMO Systems over Composite RG Fading Channels," *AEU-International J. Electron. and Commun.*, vol. 88, pp. 134-140, 2018. Article (CrossRef Link).

[28] K. Guo, D. Guo, B. Zhang, and Y. Huang, "Outage analysis and impairments allocation of two-way opportunistic relaying network with hardware impairments," in *Proc. of 2016 IEEE/CIC International Conference on Commun. China (ICCC)*, Jul. 2016, pp. 1–6. Article (CrossRef Link).

[29] X. Li, J. Li, Y. Liu, Z. Ding, and A. Nallanathan, "Outage Performance of Cooperative NOMA Networks with Hardware Impairments," in *Proc. of IEEE Global Communications Conference (GLOBECOM'18)*, Jul. 2018. Article (CrossRef Link)

[30] M. Matthaiou, A. Papadogiannis, E. Bjornson, and M. Debbah, "Two-Way Relaying Under the Presence of Relay Transceiver Hardware Impairments," *IEEE Commun. Lett.*, vol. 17, no. 6, pp. 1136–1139, Jun. 2013. Article (CrossRef Link)

[31] F. Ding, H. Wang, S. Zhang, M. Dai, "Impact of Residual Hardware Impairments on Non-Orthogonal Multiple Access Based Amplify-and-Forward Relaying Networks," *IEEE Access*, vol. 6, pp. 15117–15131, 2018. Article (CrossRef Link)

[32] M. Medard, "The effect upon channel capacity in wireless communications of perfect and imperfect knowledge of the channel," *IEEE Trans. Inf. Theory*, vol. 46, no. 3, pp. 933–946, May 2000. Article (CrossRef Link)

[33] X. Zhang, M. Matthaiou, M. Coldrey, and E. Bjo¨rnson, "Impact of Residual Transmit RF Impairments on Training-Based MIMO Systems," *IEEE Trans. Commun.*, vol. 63, no. 8, pp. 2899–2911, Aug. 2015. Article (CrossRef Link)

[34] X. Yue, Y. Liu, S. Kang, and A. Nallanathan, "Performance Analysis of NOMA With Fixed Gain Relaying Over Nakagami-m Fading Channels," *IEEE Access*, vol. 5, pp. 5445–5454, 2017. Article (CrossRef Link)

[35] S. Nadarajah, "A Review of Results on Sums of Random Variables," *Acta Apple Math*, vol. 103, pp. 131–140, sep. 2008. Article (CrossRef Link)

Xinji Tian was born in Henan, china, in 1983. She received Ph.d. degree in signal and information processing from Beijing university of Posts and Telecommunications (BUPT), China in 2011. she is Currently working as Associate professor in School of Physics and Electronic Information Engineering, Henan Polytechnic University. Her research interests include wireless communication, massive MIMO, non-orthogonal multiple access, ultra-dense network.

Qianqian Li received the B.Sc degree in communication engineering from the College of Information Engineering, Zhengzhou Shengda University, in 2016. She is currently pursuing the M.Sc. degree in communication and information systems with the School of Physics and Electronic Information Engineering, Henan Polytechnic University, Jiaozuo China. Her current research interests include nonorthogonal multiple access and hardware constrained communication.

Xingwang Li (S'12-M'15) received his B.Sc. degree in communication engineering from Henan Polytechnic University, China, in 2007. He then received the M. Sc. degree from the National Key Laboratory of Science and Technology on Communications at University of Electronic Science and Technology of China (UESTC), in 2010 and Ph. D. degrees in communication and information system from the State Key Laboratory of Networking and Switching Technology at Beijing University of Posts and Telecommunications (BUPT), in 2015. From 2010 to 2012, he was with Comba Telecom Ltd. in Guangzhou China, as a engineer. He spent one year from 2017 to 2018 as a visiting scholar at the Institute of Electronics, Communications and Information Technology (ECIT), Queen's University Belfast (QUB), Belfast, UK. He is currently Associated Professor with the School of Physics and Electronic Information Engineering, Henan Polytechnic University, Jiaozuo China. He has several papers published in journal and conferences, has authored several patents and he has worked on several funded research projects on the wireless communications areas. His research interests include MIMO communication, cooperative communication, hardware constrained communication, non-orthogonal multiple access, physical layer security, unmanned aerial vehicles, free space optical communications, and performance analysis of fading channels. Dr. Li now serves as an editor of the KSII Transactions on Internet and Information Systems and TPC member of IEEE/CIC ICCC workshop. 19', He also has served a TPC member of IEEE Globecom Workshop. 18'.

Hui Zhang received his B.Sc. degree in communication engineering from Henan Polytechnic University, China, in 2007. He then received the M. Sc. degree from the School of Energy Science and Engineering, Henan Polytechnic University, in 2010 and Ph. D. degrees from the School of Energy and Mining Engineering, China University of Mining and Technology, in 2013. He is currently a Associated Professor with the School of Energy Science and Engineering, Henan Polytechnic University. He has authored several papers in journal and conferences and holds several patents. His research interests include mining communication and smart mine.

Khaled M. Rabie received the B.Sc. degree (Hons.) in electrical and electronic engineering from the University of Tripoli, Tripoli, Libya, in 2008, and the M.Sc. and Ph.D. degrees in communication engineering from The University of Manchester, Manchester, U.K., in 2010 and 2015, respectively. He is currently a Post-Doctoral Research Associate with Manchester Metropolitan University (MMU), Manchester. His research interests include signal processing and the analysis of power line and wireless communication networks. He was a recipient of the Best Student Paper Award at the IEEE ISPLC, TX, USA, 2015, and the MMU Outstanding Knowledge Exchange Project Award of 2016. He is currently the Program Chair of the IEEE ISPLC 2018, the IEEE CSNDSP 2018 Co-Chair of the Green Communications and Networks track, and the Publicity Chair of the INISCOM 2018. He is also an Associate Editor of the IEEE ACCESS, an Editor of the Physical Communication journal (Elsevier), and a fellow of the U.K. Higher Education Academy.

Charles Casimiro Cavalcante received the B.Sc and M.Sc in Electrical Engineering from the Federal University of Cear (UFC), Brazil, in 1999 and 2001, respectively, and the Ph.D. degree from the University of Campinas (UNICAMP), Brazil, in 2004. He has held a grant for Scientific and Technological Development from 2004 to 2007 and since March 2009 he has a grant of Scientific Research Productivity both from the Brazilian Research Council (CNPq). From March 2007 to November 2008 he was a Visiting Professor at Teleinformatics Engineering Department of UFC and since November 2008 he is an Assistant Professor at the same department and university holding the Statistical Signal Processing chair. From August 2014 to July 2015 he was a Visiting Assistant Professor at the Department of Computer Science and Electrical Engineering (CSEE) from University of Maryland, Baltimore County (UMBC) in the United States. He has been working on signal processing strategies for communications where he has several papers published in journal and conferences, has authored three international patents and he has worked on several funded research projects on the signal processing and wireless communications areas. He is also a co-author of the book Unsupervised Signal Processing: Channel Equalization and Source Separation, published by CRC Press. He is a researcher of the Wireless Telecommunications Research Group (GTEL) where he leads research on signal processing and wireless communications. Dr. Cavalcante is a Senior Member of the IEEE and Senior Member of the Brazilian Telecommunications Society (SBrT). His main research interests are in signal processing for communications, blind source separation, wireless communications, and statistical signal processing